

## Effect of magnetic fields on spin glass dynamics

Qiang Zhai,<sup>1,\*</sup> David C. Harrison,<sup>2</sup> and Raymond L. Orbach<sup>1,†</sup>

<sup>1</sup>*Texas Materials Institute, The University of Texas at Austin, Austin, Texas 78712, USA*

<sup>2</sup>*School of Physics and Astronomy, The University of Minnesota, Minneapolis, Minnesota 55455, USA*

(Received 28 May 2017; revised manuscript received 19 July 2017; published 7 August 2017)

The effects of a magnetic field on spin glass dynamics are explored for a  $\text{Cu}_{0.887}\text{Mn}_{0.113}$  thin film of thickness  $\mathcal{L} = 20$  nm in a multilayer configuration. An experimental protocol removes uncertainties associated with the time dependence of the field-cooled magnetization  $M_{\text{FC}}(t, T)$ . Activated dynamics is exhibited after the spin glass correlation length  $\xi(t, T)$  has reached  $\mathcal{L}$ , creating a quasiequilibrium state. The activation energy depends upon the strength of the magnetic field  $H$ . The magnitude of the activation energy diminishes as  $H^2$ , the coefficient of which is proportional to the number of correlated spins. A quantitative fit requires a “pancakelike” correlated region, associated with the  $T = 0$  phase transition for a spin glass in  $D = 2$  dimensions.

DOI: [10.1103/PhysRevB.96.054408](https://doi.org/10.1103/PhysRevB.96.054408)

### I. INTRODUCTION

The effect of a magnetic field on spin glass dynamics has been an issue of dispute for nearly 30 years. The Parisi mean-field solution [1] of the infinite range Sherrington-Kirkpatrick model [2] predicts a phase transition at a “glass temperature”  $T_g(H)$  that depends upon the magnitude of the magnetic field [3]. The “droplet model”, formulated by Fisher and Huse, finds “...the ordered phase is unstable to a uniform (or random) magnetic field and no long-range spin-glass ordering occurs in the presence of a magnetic field” [4]. An explicit test of these divergent perspectives was performed by Lefloch *et al.* [5]. They measured the properties of the  $\text{CdCr}_{1.7}\text{In}_{0.3}\text{S}_4$  spin glass in a magnetic field. Their experiments displayed a field-temperature phase diagram “...reminiscent of the mean field result for the infinite range model with finite anisotropy...”. Their study concluded with the following observation: “Thus, even if the spin glass does not exist in a magnetic field, at least it looks the same as in zero field, as far as we experimentalists can see”.

The purpose of this paper is to explore the effects of magnetic fields on the dynamics of the canonical spin glass CuMn. Previous work reported similar experiments on an amorphous GeMn thin film [6]. The present investigation extends their study to a more conventional spin glass, and provides a quantitative analysis of the nature of the correlated region (see below). In addition, it extends the experimental protocol of Ref. [6] to the case where the field-cooled magnetization  $M_{\text{FC}}(t, T)$  is time dependent, as it is for CuMn thin films.

The concept of the growth of a spin glass correlation function with time  $t$  at temperature  $T$ ,  $\xi(t, T)$ , is common to both of the conflicting models for spin glass dynamics. It is assumed that the spin glass is quenched from a temperature above the spin glass transition temperature  $T_g$  to a temperature  $T < T_g$ . Upon the quench, spin glass order is nucleated at a given site, and grows with time. Numerical simulations [7] find a power law growth,

$$\xi(t, T) = c_1 a_0 \left( \frac{t}{\tau_0} \right)^{c_2(T/T_g)}, \quad (1)$$

where  $c_1$  and  $c_2$  are constants of order unity and 0.1, respectively,  $a_0$  is an average distance between the moments making up the spin glass material, and  $\tau_0$  is an exchange time of the order of  $\hbar/k_B T_g$ . As  $\xi(t, T)$  grows, there are ever increasing free-energy barriers encountered, with heights  $\Delta(t, T)$  given by [8]

$$\frac{\Delta(t, T)}{k_B T_g} = \frac{1}{c_2} \left[ \ln \left( \frac{\xi(t, T)}{a_0} \right) - \ln c_1 \right]. \quad (2)$$

The droplet model [4] assumes activated growth and finds

$$\xi(t, T) = \alpha a_0 \left[ \left( \frac{T}{T_g} \right) \ln \left( \frac{t}{\tau_0} \right) \right]^{1/\psi}, \quad (3)$$

where  $\alpha$  is a constant of order unity, and  $\psi$  is a critical exponent. Similar to power law growth, there are ever increasing free-energy barriers encountered, with height,

$$\frac{\Delta(t, T)}{k_B T_g} = \left( \frac{\xi(t, T)}{\alpha a_0} \right)^\psi. \quad (4)$$

For experiments on bulk samples,  $\xi(t, T)$  grows indefinitely, so that any measurement over a time interval is “chasing” an ever increasing correlation length, and concomitantly, ever increasing free-energy barrier heights. The beauty of working with thin films at the “mesoscale” is that the growth of  $\xi(t, T)$  perpendicular to the plane of the film stops when  $\xi_\perp(t, T) = \mathcal{L}$ . At this point in time, the spin glass system crosses over from  $D = 3$  to  $D = 2$  dimensions. As known theoretically [9] and shown experimentally [10], the lower critical dimension for spin glasses  $2 < d_\ell < 3$  (a recent theoretical value [11] finds  $d_\ell = 2.5$ ). This results in  $T_g = 0$  for the spin glass, with critical fluctuations at temperature  $T$  leading to an equilibrium  $D = 2$  parallel correlation length of  $\xi_\parallel \approx a_0 T^{-\nu_{2d}}$ . Recent calculations [12] for Ising spin glasses have established  $\nu_{2d} = 3.53$ . Previously, Kawamura and Yonehara [13] found for a Heisenberg spin glass  $\nu_{2d} = 0.9 \pm 0.2$  for the spin correlation length, and  $\nu_{2d} = 2.1 \pm 0.3$  for the chiral correlation length. While CuMn normally is regarded as a Heisenberg spin glass, sufficient anisotropy can mimic Ising-like behavior [14]. It will turn out (see below) that our final result will be relatively insensitive to the precise value of  $\nu_{2d}$ .

It would be tempting to set quantitatively an equilibrium value for  $\xi_\parallel = a_0 (T_g/T)^{\nu_{2d}}$ . However, this would ignore the

\*qiang@utexas.edu

†orbach@mail.utexas.edu

spin glass correlations that have been built up while  $\xi(t, T)$  has been growing to reach  $\mathcal{L}$ . One can intuitively think of a “renormalization” of the length scale for the correlated spins from  $a_0$  to  $\mathcal{L}$ . This would then lead to a multiplicative relationship for the equilibrium value of the parallel correlation length  $\xi_{\parallel}(t, T)$ , first suggested by Young [15] and amplified by Martin-Mayor [16], changing  $\xi_{\parallel} = a_0(T_g/T)^{\nu_{2d}}$  to

$$\xi_{\parallel}(T) = k(T)\mathcal{L} = b\left(\frac{T_g}{T}\right)^{\nu_{2d}} \mathcal{L}, \quad (5)$$

where  $b$  is a scaling coefficient of order unity. An unresolved issue is the time dependence of the growth of  $\xi_{\parallel}(t, T)$  to its equilibrium value. We have no way of assessing this time scale, but the magnetic field effect on the dynamics when  $\xi_{\perp}(t, T)$  has reached  $\mathcal{L}$  (see below) appears to be independent of time. This suggests that the growth of  $\xi_{\parallel}(t, T)$  is sufficiently rapid that it has reached its equilibrium value when  $\xi_{\perp}(t, T)$  has reached  $\mathcal{L}$ .

With these assumptions, we can define a “crossover time”  $t_{\text{co}}$  by the relationship

$$\xi_{\perp}(t_{\text{co}}, T) = \mathcal{L}. \quad (6)$$

Both models then suggest that there is a maximum free-energy barrier height  $\Delta_{\text{max}}(\mathcal{L})$  that governs the dynamics for  $t > t_{\text{co}}$ . It is tempting to extract the maximum free-energy barrier from Eqs. (2) and (4) by simply substituting  $\mathcal{L}$  for  $\xi(t_{\text{co}}, T)$  in the respective equations. However, both are derived assuming a spherical correlated volume which, as we shall show below, is not the case given that  $\xi_{\parallel}(T) > \xi_{\perp}(t_{\text{co}}, T)$ . In our subsequent analysis, we shall extract the value of  $\Delta_{\text{max}}(\mathcal{L})$  as a function of magnetic field  $H$  from the time decay of the measured magnetizations. The proportionality will turn out to depend upon  $H^2$ . The coefficient of  $H^2$  will be the number of spins correlated in the spin glass state for times greater than  $t_{\text{co}}$ , times the measured susceptibility per spin. Experiments will favor their containment in a “pancakelike” volume of perpendicular height  $\mathcal{L}$  and parallel radius  $\xi_{\parallel}(T)$ .

The effects of magnetic fields on spin glass dynamics will be outlined in the next section. The sample preparation and experimental protocol will be described in Sec. III. The latter will be different from that used in our previous investigation [6,17], because the field-cooled magnetization in CuMn thin films is time dependent, as noted in previous work [18], complicating the extraction of the irreversible magnetization. The experimental results will be presented in Sec. IV, and their analysis in Sec. V. Section VI contains the summary and conclusions.

## II. EFFECTS OF A MAGNETIC FIELD ON SPIN GLASS DYNAMICS

Earlier work [6,8,19,20] has shown that an applied magnetic field reduces the barrier heights in a spin glass according to the strength of the Zeeman interaction upon the correlated states  $E_Z$ . Simply stated,

$$\Delta_{\text{max}}(H, \mathcal{L}) \rightarrow \Delta_{\text{max}}(\mathcal{L}) - E_Z. \quad (7)$$

There is a dispute in the literature about the magnitude for  $E_Z$ , and its dependence upon magnetic field strength. A “trap model” [19] postulates the reduction of the depth of an effective

trap by a Zeeman energy arising from fluctuations in the number of correlated spins, proportional to  $\sqrt{N_c}$  and linear in  $H$ , where  $N_c$  is the number of correlated spins. A barrier model [8] takes the Zeeman energy to be equal to the magnetic susceptibility per spin  $M_{\text{FC}}/N_s$  times  $N_c$  and  $H^2$ , where  $M_{\text{FC}}$  is the field-cooled magnetization of the sample, and  $N_s$  the total number of spins in the sample. Reference [6] shows that, for the strengths of magnetic fields used in these experiments, the latter dominates the former by almost two orders of magnitude. For that reason, we set

$$E_Z = N_c \chi_{\text{FC}} H^2, \quad (8)$$

where  $\chi_{\text{FC}}$  is the measured magnetic susceptibility per spin. As will be discussed in Sec. V, there is also a contribution from the diamagnetism of the Cu in the multilayer sample. This is shown to be two orders of magnitude smaller than the contribution from the Mn moments in the spin glass state.

Experimentally, if upon quenching the temperature to  $T < T_g$ , one waits for times greater than  $t_{\text{co}}$ , the correlation lengths will be pinned at  $\xi_{\perp} = \mathcal{L}$  and  $\xi_{\parallel}(T)$  from Eq. (5). The dynamics is determined by the largest barrier height in both models, so that, with the correlation length pinned,  $\Delta_{\text{max}}(\mathcal{L})$  in Eq. (7) is a constant. This leads to activated dynamics, with the activation energy now a function of magnetic field as a consequence of Eqs. (7) and (8). Thus, by observing activated magnetization dynamics for  $t > t_{\text{co}}$  as a function of magnetic field, one can extract  $E_Z$  and hence both the power of  $H$  and its coefficient. The latter will be proportional to the number of correlated spins  $N_c$ , allowing a quantitative estimate for  $E_Z$  from Eqs. (5) and (6).

## III. SAMPLE PREPARATION AND EXPERIMENTAL PROTOCOL

The CuMn thin film multilayer sample was prepared at the University of Minnesota by dc sputtering 99.9% CuMn/99.999% Cu multilayers at an argon pressure of 2 mTorr. The multilayers have an alternating structure of 20 nm CuMn and 60 nm Cu, in order to achieve amplification of the signal magnitude, and to decouple the spin glass moments between layers. Two 1- $\mu\text{m}$ -thick CuMn films from separate targets were synthesized, yielding a “bulk” glass transition temperature  $T_g$  of  $54 \pm 1$  and  $52 \pm 1$  K, respectively. The nominal Mn concentration of the CuMn target was 13.5 at. %. Scaling with respect to  $T_g$  [21,22] translates the Mn concentration in the multilayers to  $\approx 11.7$  at. %.

The measurements of the zero-field-cooled magnetization  $M_{\text{ZFC}}(t, T)$  for the 20.0 nm CuMn multilayer would normally have followed the protocol [6] developed in a previous paper. The introduction of a protocol different from conventional measurements of  $M_{\text{ZFC}}(t, T)$  is a consequence of the time dependence of the field-cooled magnetization  $M_{\text{FC}}(t, T)$  for mesoscale CuMn films. Whereas in bulk,  $M_{\text{FC}}(t, T)$  varies little, and, if anything, slightly *diminishes* with increasing measurement time [23], at the mesoscale it *increases* rather substantially with increasing measurement time [17]. We believe this is a consequence of glassy dynamics. As shown previously, irreversibility sets in below a freezing temperature  $T_f$  for thin film spin glasses well below the bulk spin glass transition temperature  $T_g$ . As shown in Ref. [17], this is

because of a largest barrier height  $\Delta_{\max}(\mathcal{L})$  in mesoscopic spin glasses. A finite experimental time scale  $\tau_{\text{expt.}}$  sets  $T_f$  by the relationship

$$\frac{1}{\tau_{\text{expt.}}} \approx \frac{1}{\tau_0} \exp(-\Delta_{\max}/k_B T_f), \quad (9)$$

where  $\tau_0$  is an exchange time of the order of  $\hbar/k_B T_g$ . This relationship suggests that the longer the experimental time scale, the lower is the value of  $T_f$ , but for  $T > T_f$ , the magnetization is *increasing* as  $T$  is lowered (i.e., along the Curie-Weiss trajectory). Hence, at a longer measurement time scale,  $T_f$  is lower, and the irreversible magnetization is larger at the lower temperature, but the magnetization at the onset of irreversibility is just the field-cooled magnetization  $M_{\text{FC}}(t, T)$ . The increase of  $M_{\text{FC}}(t, T)$  with time is not an intrinsic behavior, but rather arises from the glassy dynamics of mesoscopic spin glasses.

Because the irreversible magnetization is the difference between between  $M_{\text{ZFC}}(t, T)$  and  $M_{\text{FC}}(t, T)$ , both must be measured over the same time and temperature profile when the latter is time dependent. Previous work was performed at a fixed magnetic field. Measuring the magnetic field dependence of  $\Delta_{\max}(H)$  requires multiple measurements at different fields. The previous protocol proved to be too cumbersome to be practical.

Instead, we developed a protocol in which  $M_{\text{FC}}(t, T)$  cancels out. Two symmetrical magnetization decays, the zero-field-cooled magnetization  $M_{\text{ZFC}}(t, T)$  and the thermoremanent magnetization  $M_{\text{TRM}}(t, T)$ , were performed in the presence of a magnetic field. The irreversible magnetization is derived from both procedures,

$$M_{\text{IRR}}(t, T) = M_{\text{FC}}(t, T) - M_{\text{ZFC}}(t, T), \quad (10)$$

a standard relationship. Also,

$$M_{\text{IRR}}(t, T) = M_{\text{TRM}}(t, T) - M_{\text{FC}}(t, T), \quad (11)$$

which is required if the decay takes place in a magnetic field, where  $M_{\text{FC}}(t, T)$  is time dependent. The protocol is as follows.

The “ $M_{\text{ZFC}}(t, T)$ ” is measured by quenching the sample from above  $T_g$  to a temperature  $T$  in a magnetic field  $H - \delta H$ . As soon as the temperature stabilizes, the magnetic field is increased abruptly to  $H$  and the “new” zero-field magnetization is measured as a function of time. Concomitantly, the sample is warmed up above  $T_g$ , and a magnetic field  $H + \delta H$  is applied. The sample temperature is then quenched in the presence of this field to a temperature  $T$ . After temperature stabilization, the magnetic field is reduced to  $H$  and a “new” thermoremanent magnetization is measured as a function of time. The important point of these procedures is that both the zero-field-cooled and thermoremanent magnetizations are measured in the *same* magnetic field  $H$ . From Eqs. (10) and (11), this means that  $M_{\text{FC}}(t, T)$  is the same for both measurements. Hence, adding Eqs. (10) and (11) cancels the time-dependent field-cooled magnetization. We have, therefore,

$$M_{\text{IRR}}(t, T) = \frac{1}{2}[M_{\text{TRM}}(t, T) - M_{\text{ZFC}}(t, T)]. \quad (12)$$

We use this protocol in the following section to extract the magnetic field dependence of the maximum barrier height  $\Delta_{\max}(H, \mathcal{L})$ .

#### IV. EXPERIMENTAL RESULTS

The protocol described in the previous section was carried out for the 20 nm CuMn multilayered sample described therein. The incremental field  $\delta H$  was set at 20 G, and measurement fields  $H$  were applied over a range from  $30 \leq H \leq 144$  G.  $M_{\text{IRR}}(t, T)$ , defined in Eq. (12), was then measured over a large time range. The value of  $\Delta_{\max}(H, \mathcal{L})$  was extracted by measuring the slope of the  $\ln M_{\text{IRR}}(t, T)$  vs  $t$  for times  $t > t_{\text{co}}$ . A difficulty arises from the relationship between the crossover time  $t_{\text{co}}$  and the field-dependent maximum barrier height  $\Delta_{\max}(H, \mathcal{L})$ ,

$$t_{\text{co}} = \tau_0 \exp[\Delta_{\max}(H, \mathcal{L})/k_B T]. \quad (13)$$

The variation of  $t_{\text{co}}$ , as a consequence of the change in  $\Delta_{\max}(H, T)$  for different values of  $H$ , is sufficient to require that the extraction of  $M_{\text{IRR}}(t, T)$  be carried out at different temperatures. Previous work [6] has shown that  $\Delta_{\max}(\mathcal{L})$  is independent of temperature.

Representative experimental data are exhibited in Fig. 1. The crossover time is indicated by an arrow, and the solid line a fit to activated decay with activation energy  $\Delta_{\max}(H, \mathcal{L})$ . Looking at the data, it may not seem obvious where to identify the activated region. Noting the dependence of  $t_{\text{co}}$  on  $\Delta_{\max}(H, \mathcal{L})$  from Eq. (13), one sees that there is a coupling between  $t_{\text{co}}$  and the slope. The two are adjusted until they are consistent. This minimizes the error in the evaluation of  $\Delta_{\max}(H, \mathcal{L})$ . The values extracted in this manner are listed in Table I.

Now that the values of  $\Delta_{\max}(H, \mathcal{L})$  have been determined, they can be plotted against  $H^2$  to determine the validity of Eq. (8). Figure 2 is a plot of the data contained in Table I, with a least-squares fit line displaying the proportionality to  $H^2$ . One finds

$$\Delta_{\max}(H, \mathcal{L})/k_B = \Delta_{\max}(0, \mathcal{L})/k_B - \alpha H^2, \quad (14)$$

with  $\alpha$  lying between  $3.21 \times 10^{-3}$  and  $6.02 \times 10^{-3}$ , with a most probable value of  $4.61 \times 10^{-3}$ . The magnitude of  $\alpha$ , proportional to the number of correlated spins, will be examined in the next section.

#### V. ANALYSIS OF EXPERIMENTAL RESULTS

The reduction of  $\Delta_{\max}(H, \mathcal{L})$  in the presence of a magnetic field, as given in Eq. (14), has the form

$$\alpha H^2 = N_c \chi_s H^2 / k_B, \quad (15)$$

where  $N_c$  is the number of correlated spins (i.e., enclosed in the correlated volume), and  $\chi_s$  is the magnetic susceptibility per spin. The total magnetization of the sample is the sum of the Mn spin glass moment plus the diamagnetic magnetization of the Cu, from both in the CuMn films and in the intervening layers. Designating the component from the Mn spin glass as  $M_{\text{sg}}$  and that from the Cu as  $M_{\text{Cu}}$ , we have

$$\chi_s = \frac{M_{\text{sg}}}{H V_\ell \lambda / V_s}, \quad (16)$$

where  $V_\ell$  is the volume of a given layer of CuMn,  $\lambda$  is the number of CuMn layers, and  $V_s$  is the volume/spin. The number of correlated spins  $N_c = V_c / V_s$ , where  $V_c$  is the

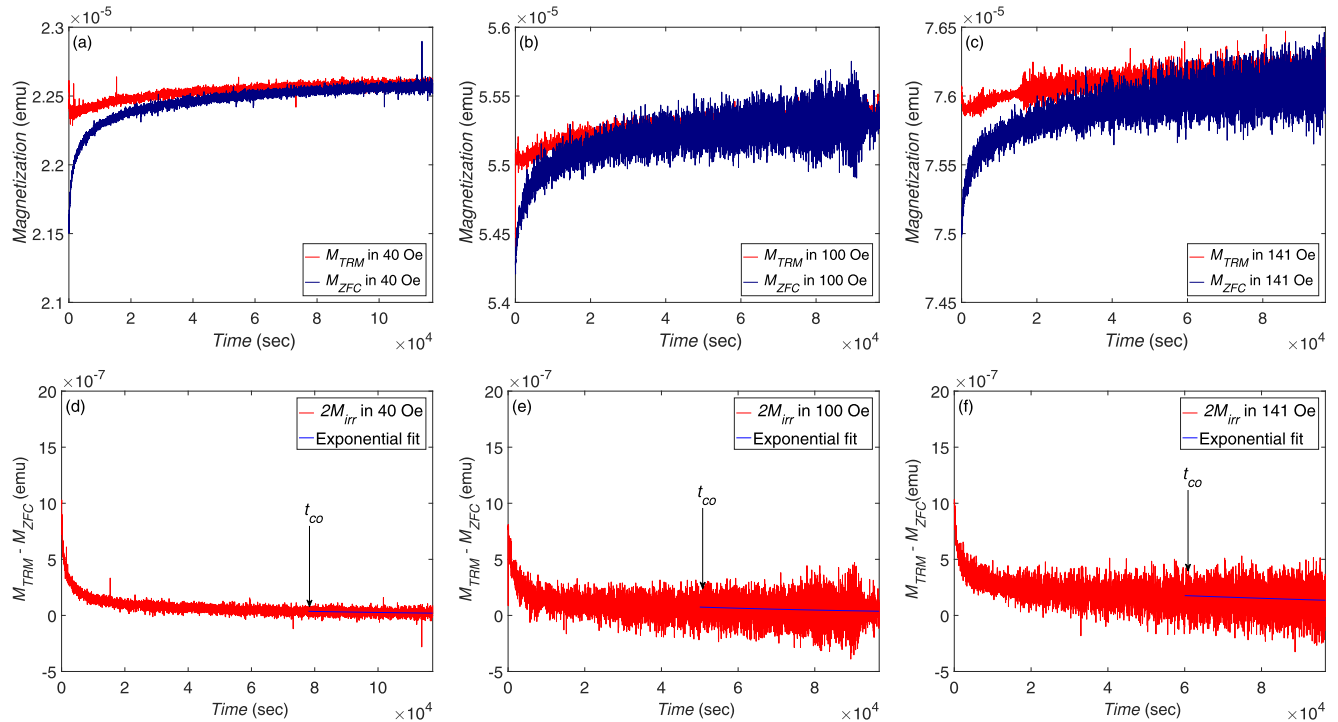


FIG. 1. (a)–(c) The measured magnetizations  $M_{TRM}(t, T)$  and  $M_{ZFC}(t, T)$  plotted against time for a 20 nm CuMn multilayer thin film at representative fields. Initially, for very short times,  $M_{TRM}(t, T)$  does decay as it would normally in a bulk material. However, because of the growth of  $M_{FC}(t, T)$  with time,  $M_{TRM}(t, T)$  increases for times beyond the short initial decay time. This can be seen if one looks closely near the zero of time in the (a)–(c) plots. (d)–(f)  $2M_{IRR} = M_{TRM}(t, T) - M_{ZFC}(t, T)$  and its fit to activated dynamics. (a), (d) At 42 K in 40 Oe, (b), (e) at 41 K in 100 Oe, and (c), (f) at 40 K in 141 Oe.

volume containing the correlated spins. Then  $\alpha$  is given by

$$\alpha = N_s \chi_s / k_B = \frac{V_c}{V_s} \frac{M_{sg}}{(H V_\ell \lambda / V_s) k_B} = \frac{1}{k_B} \frac{M_{sg}}{H} \frac{V_c}{V_\ell \lambda}. \quad (17)$$

The measured magnetization is the sum of  $M_{sg}$  and that from the Cu. The latter is given by [24]

$$\chi_{Cu} = \left( -0.093 + \frac{0.023}{T} \right) \times 10^{-6} \text{ cm}^3 \text{ g}^{-1}. \quad (18)$$

At our measuring temperature range,  $T \approx 40$  K,  $\chi_{Cu} = -0.0824 \times 10^{-6} \text{ cm}^3/\text{g}$ . The Cu magnetization is then given by  $M_{Cu} = \chi_{Cu} V_{Cu} \rho H$ , where  $V_{Cu}$  is the total volume of Cu in the multilayer, and  $\rho$  is the Cu mass density.

The relative contributions of the Mn moments in the spin glass state to that of the Cu are calculated for a magnetic

TABLE I.  $\Delta_{\max}(H, \mathcal{L})/k_B$  extracted at different fields for the 20 nm CuMn thin film.

$H$ (Oe)	$T$ (K)	$\Delta_{\max}(H, \mathcal{L})/k_B$ (K)
30	42	$1732 \pm 21$
40	42	$1715 \pm 8$
55	42	$1710 \pm 10$
80	41.5	$1700 \pm 30$
100	41	$1668 \pm 17$
122.5	41	$1670 \pm 24$
144	40	$1631 \pm 18$

field of  $H = 141$  G. The cross-section dimension of the multilayer is approximately  $2.3 \text{ cm} \times 2.3 \text{ cm}$ . Putting in all the relevant dimensions, we calculate a total Cu magnetization  $M_{Cu} = -1.70 \times 10^{-7} \text{ emu}$ . The measured magnetization is  $M_{\text{tot}} = 7.61 \times 10^{-5} \text{ emu}$ . Hence, the Cu diamagnetism is two orders of magnitude smaller than the measured magnetization.

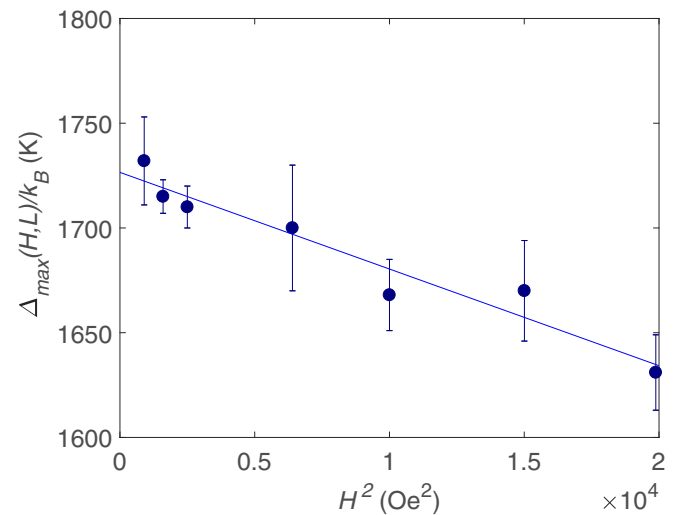


FIG. 2. A plot of the extracted values for  $\Delta_{\max}(H, \mathcal{L})/k_B$  as a function of  $H^2$  and its least-squares fit in the form of  $\Delta_{\max}(H, \mathcal{L})/k_B = \Delta_{\max}(0, \mathcal{L})/k_B - \alpha H^2$ , for  $\alpha \approx 4.61 \times 10^{-3}$ .



We wish to find the correlated volume  $V_c$  in order to find the number of correlated spins from the measured magnetization using Eq. (16). There are two possibilities: either a spherical volume (no further growth in the parallel direction once the perpendicular correlation length has reached  $\mathcal{L}$ ), or a pancakelike shape allowing for an equilibrium multiplicative growth in the parallel direction.

For a spherical correlated volume,

$$V_c = \frac{4}{3}\pi \left(\frac{\mathcal{L}}{2}\right)^3. \quad (19)$$

Putting in the quantities in Eq. (17), we find  $\alpha = 3.9 \times 10^{-5}$ , about two orders of magnitude less than the measured value.

For the pancake shape, the correlated volume from Eqs. (5) and (6) is given by

$$V_c = \pi b^2 \mathcal{L}^3 \left(\frac{T_g}{T}\right)^{2\nu_{2d}}. \quad (20)$$

Inserting this expression for  $V_c$  into Eq. (17), and using the value of  $\alpha = 4.61 \times 10^{-3}$  from experiments (taking  $T_g = 53$  K), generates an expression for the scaling coefficient  $b$  that depends upon the choice of exponent  $\nu_{2d}$ . Using the values associated with Ising, Heisenberg spin, or chiral correlation lengths, we find  $b = 1.6, 3.45,$  or  $2.46$ , respectively. For a coefficient  $b$  “of order of unity” it would appear that Ising-like growth is present, but clearly Heisenberg or chiral correlation length growth cannot be ruled out. In our case, it seems clear that our experimental results are best satisfied with a pancakelike correlated structure as a consequence of  $D = 2$  spin glass dynamics.

As a final note, we have assumed compact growth for the number  $N_c$  of correlated spins in Eqs. (19) and (20). As pointed out in Ref. [20], the correlated space is in fact fractal, with a dimensionality exponent of  $\sim 2.81$  instead of 3. This has the effect of replacing  $\mathcal{L}^3$  in Eqs. (19) and (20) by  $\mathcal{L}^{2.81}$ , thereby increasing  $b$  concomitantly for the pancakelike correlated structure. For Ising, Heisenberg spin, or chiral correlation length growth, we find  $b = 2.73, 5.71,$  or  $4.08$ , respectively, again favoring Ising-like growth, but with Heisenberg spin or chiral still a possibility. A direct test of compact versus fractal growth would be a set of experiments similar to those contained in this paper, but with differing thin film thicknesses. By varying  $\mathcal{L}$ , and measuring the coefficient of the  $H^2$  reduction in  $\Delta_{\max}(H, \mathcal{L})$ , one can uniquely detect the difference between

compact and fractal growth through the measured exponent of  $\mathcal{L}$  in Eq. (20). The relatively small value of the changes in  $\Delta_{\max}(H, \mathcal{L})/k_B$  exhibited in Table I make this a somewhat daunting, but still possible, task.

## VI. SUMMARY AND CONCLUSIONS

We have measured the effects of magnetic fields upon the dynamics of the canonical spin glass CuMn. By using thin films of thickness 20 nm, contained in a multilayer structure with intervening Cu layers for interlayer decoupling, we have been able to “freeze” the growth of the spin glass correlation length  $\xi(t, T)$ . This has enabled a direct measure of the reduction of the free-energy barrier heights with increasing magnetic field. We have been able to extract a quantitative estimate of this effect, and compared it with calculations of the number of correlated spins participating in the dynamics.

Comparing the consequences of the growth of  $\xi(t, T)$  in the perpendicular and parallel directions, we have been able to exhibit the importance of fluctuations associated with a  $T = 0$  transition temperature for a spin glass in  $D = 2$ . With a reasonable value for the scaling factor, we have shown the stable shape of the correlated region to have a “pancakelike” shape, with the perpendicular dimension  $\mathcal{L}$  of the film thickness, and a parallel dimension exhibiting a multiplicative correlation appropriate to the equilibrium value of the  $D = 2$  correlation function at the measurement temperature.

Future measurements on CuMn films of different thicknesses will test further properties of the growth of  $\xi(t, T)$ . For example, is the growth of the correlated regions compact or fractal [20]? Now that the scaling factor  $b$  has been fixed, it should be possible to compare the number of correlated spins as a function of film thickness  $\mathcal{L}$ , and in that way determine the nature of the growth of  $\xi(t, T)$ . It would also be interesting to explore other spin glass systems to test for the universality of these results.

## ACKNOWLEDGMENTS

We thank Dr. Victor Martin-Mayor for many helpful conversations. This work was supported by the US Department of Energy, Office of Basic Energy Sciences, Division of Materials Science and Engineering, under Award No. DE-SC0013599.

- 
- [1] G. Parisi, *Phys. Lett. A* **73**, 203 (1979); *Phys. Rev. Lett.* **43**, 1754 (1979); *J. Phys. A* **13**, L115 (1980); M. Mézard, G. Parisi, N. Sourlas, G. Toulouse, and M. Virasoro, *J. Phys. (Paris)* **45**, 843 (1984); M. Mézard and M. A. Virasoro, *ibid.* **46**, 1293 (1985).
  - [2] D. Sherrington and S. Kirkpatrick, *Phys. Rev. Lett.* **35**, 1792 (1975).
  - [3] J. De Almeida and D. J. Thouless, *J. Phys. A* **11**, 983 (1978).
  - [4] D. S. Fisher and D. A. Huse, *Phys. Rev. Lett.* **56**, 1601 (1986); D. A. Huse and D. S. Fisher, *J. Phys. A* **20**, L997 (1987); D. S. Fisher and D. A. Huse, *Phys. Rev. B* **36**, 8937 (1987); **38**, 373 (1988); **38**, 386 (1988).
  - [5] F. Lefloch, J. Hammann, M. Ocio, and E. Vincent, *Physica B (Amsterdam)* **203**, 63 (1994).
  - [6] S. Guchhait and R. L. Orbach, *Phys. Rev. Lett.* **118**, 157203 (2017).
  - [7] E. Marinari, G. Parisi, J. Ruiz-Lorenzo, and F. Ritort, *Phys. Rev. Lett.* **76**, 843 (1996); J. Kisker, L. Santen, M. Schreckenberg, and H. Rieger, *Phys. Rev. B* **53**, 6418 (1996); J.-O. Andersson and P. Sibani, *Physica A (Amsterdam)* **229**, 259 (1996).
  - [8] Y. G. Joh, R. L. Orbach, G. G. Wood, J. Hammann, and E. Vincent, *Phys. Rev. Lett.* **82**, 438 (1999).
  - [9] S. Franz, G. Parisi, and M. A. Virasoro, *J. Phys. (Paris)* **I4**, 1657 (1994); L. W. Lee and A. P. Young, *Phys. Rev. B* **76**, 024405 (2007).
  - [10] S. Guchhait and R. L. Orbach, *Phys. Rev. Lett.* **112**, 126401 (2014).

- [11] S. Boettcher, *Phys. Rev. Lett.* **95**, 197205 (2005).
- [12] L. A. Fernandez, E. Marinari, V. Martin-Mayor, G. Parisi, and J. J. Ruiz-Lorenzo, *Phys. Rev. B* **94**, 024402 (2016).
- [13] H. Kawamura and H. Yonehara, *J. Phys. A* **36**, 10867 (2003).
- [14] G. F. Rodriguez, G. G. Kenning, and R. Orbach, *Phys. Rev. B* **88**, 054302 (2013).
- [15] A. P. Young (private communication, 2014).
- [16] V. Martin-Mayor (private communication, 2016).
- [17] Q. Zhai, D. C. Harrison, D. Tennant, E. D. Dalhberg, G. G. Kenning, and R. L. Orbach, *Phys. Rev. B* **95**, 054304 (2017).
- [18] L. Sandlund, P. Granberg, L. Lundgren, P. Nordblad, P. Svedlindh, J. A. Cowen, and G. G. Kenning, *Phys. Rev. B* **40**, 869 (1989).
- [19] J.-P. Bouchaud, *J. Phys. (Paris) I* **2**, 1705 (1992); E. Vincent, J.-P. Bouchaud, D. S. Dean, and J. Hammann, *Phys. Rev. B* **52**, 1050 (1995).
- [20] M. Baity-Jesi, E. Calore, A. Cruz, L. Fernandez, J. Gil-Narvion, A. Gordillo-Guerrero, D. Iñiguez, A. Maiorano, E. Marinari, V. Martin-Mayor *et al.*, *Phys. Rev. Lett.* **118**, 157202 (2017).
- [21] D. C. Vier and S. Schultz, *Phys. Rev. Lett.* **54**, 150 (1985).
- [22] U. Larsen, *Phys. Rev. B* **33**, 4803 (1986).
- [23] P. Nordblad and P. Svedlindh, Experiments on Spin Glasses, in Series on Directions in Condensed Matter Physics: Volume 12, *Spin Glasses and Random Fields*, edited by A. P. Young (World Scientific, Singapore, 1997), pp. 1–27.
- [24] R. Bowers, *Phys. Rev.* **102**, 1486 (1956).